

Numerical investigations of pile load distribution in pile group foundation subjected to vertical load and large moment

Boonchai Ukritchon^{*}, Janine Correa Faustino^a and Suraparb Keawsawasvong^b

Department of Civil Engineering, Faculty of Engineering, Chulalongkorn University, Bangkok, Thailand

(Received June 26, 2015, Revised January 18, 2016, Accepted February 03, 2016)

Abstract. This paper presents a numerical study of pile force distribution in a pile group foundation subjected to vertical load and large moment. The physical modeling of a pile foundation for a wind turbine is analyzed using 3D finite element software, PLAXIS 3D. The soil profile consists of several clay layers, which are modeled as Mohr-Coulomb material in an undrained condition. The piles in the pile group foundation are modeled as special elements called embedded pile elements. To model the problem of a pile group foundation, a small gap is created between the pile cap and underlying soil. The pile cap is modeled as a rigid plate element connected to each pile by a hinge. As a result, applied vertical load and large moment are transferred only to piles without any load sharing to underlying soil. Results of the study focus on pile load distribution for the square shape of a pile group foundation. Mathematical expression is proposed to describe pile force distribution for the cases of vertical load and large moment and purely vertical load.

Keywords: numerical analysis; finite element; pile group foundation; pile load distribution; biquartic interpolation

1. Introduction

In foundation design, shallow foundations are customarily considered first to support structural loads. If shallow foundations are not adequate and cannot satisfy requirements of settlement and bearing capacity, deep foundations are used instead to utilize the bearing capacity of stronger soil layers, which are normally located at deeper stratum. In most practical situations, piles are used in groups (pile group foundation). The layout can come in any type of geometrical pattern (square, circle, rectangle, etc.) with spacing, S (center-to-center distance between piles) for large structures. Structural loads are transferred to the pile group by means of a pile cap, which is connected to the head of each pile. When a pile group foundation is designed such that loadings are transmitted only to piles not underlying soil through contacted raft, the pile load distribution can be conventionally calculated according to most foundation handbooks (e.g., Bowles 1988, Das 2014) as

^{*}Corresponding author, Sc.D., Associate Professor, E-mail: boonchai.uk@gmail.com

^a Master's Student

^b Master's Student

$$P_k = \frac{F}{N} \pm \frac{M_y x_k}{\sum x_k^2} \pm \frac{M_x y_k}{\sum y_k^2} \quad (1)$$

where, F is the vertical applied load, N is the number of piles, M_x and M_y represents the moment about x - and y -axes respectively, x_k and y_k represents the distance of pile k from x - and y -axes, and $\sum x_k^2$ and $\sum y_k^2$ are moment of inertia of the pile group in x and y direction, respectively.

Eq. (1) stems from the assumption that the pile group foundation is modeled as a fully rigid pile cap while each pile is modeled as a spring with the same stiffness. In addition, the base of the spring must be fully rigid without any settlement, as shown in Fig. 1.

According to Eq. (1), the force distribution of each pile varies linearly with its position. For a special case of only an applied vertical load, all piles carry the same force as the average value. On the other hand, another type of analysis, the flexible pile cap, may be adopted by assuming that the pile cap may not behave rigidly but, rather, depend on its flexural stiffness, EI . Structural analysis which considers both the cap stiffness and spring stiffness must be performed for this case. As a result, the pile load distribution of a flexible cap case is different from that of a rigid cap case.

In general, the settlement of a pile group is equal to the sum of elastic shortening of the pile between cap and tip, displacement due to shearing around pile shaft, and displacement at the end bearing point, together with some interaction effects between adjacent piles. The latter is usually called the pile group effect. In order to obtain a reliable solution, pile load distribution, pile cap settlement, and soil displacement must be analyzed by numerical analyses such as the finite element method, where 3D geometry of the problem including cap and geometrical position of each pile, must be considered in the analysis.

For a pile group foundation, instead of modeling a pile as volume type, PLAXIS3D (Brinkgreve *et al.* 2013), finite element software has been developed with a special element called the embedded pile element to simulate the behavior of piles in the soil. It is composed of beam elements and interacts with the soil by means of special interface elements. The interactions of pile and soil include the skin resistance and end bearing resistance of the pile. Through the equivalent pile diameter in the material data set, the elastic zone of the pile can be determined such that the embedded pile behaves similarly as the volume pile. The mobilized side friction force and end bearing force are controlled by the limiting conditions of pile capacity as specified by users.

In recent years, a large number of previous works have been performed to study and understand

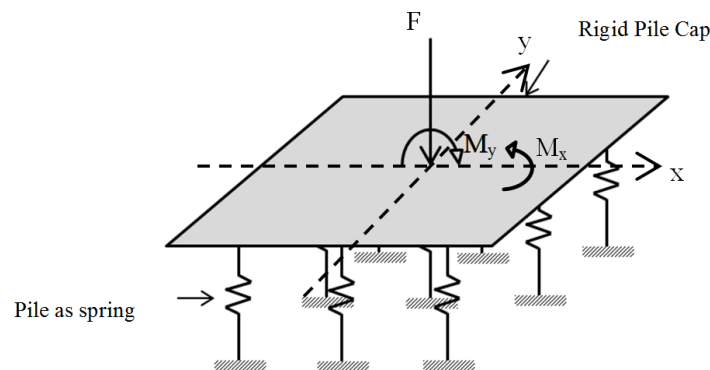


Fig. 1 Classical analysis of pile group foundation

behaviors of single pile, pile group and pile raft foundations under vertical and lateral loadings as well as their performance on static and seismic responses. Comodromos *et al.* (2003) performed a back analysis of a pile load test on the load settlement relationship of different layouts of a pile group. Their results showed that by decreasing the spacing of the piles, the interaction between them increased and, therefore, the stiffness of each pile decreased. Mandolini *et al.* (2005) studied the pile group behavior under vertical loads in terms of settlement, load distribution, and bearing capacity through monitoring full-scale structures and experimental models. They concluded that the use of classical methods for foundation design, which was used in practice, was not suitable for a proper design and needed to be revised. Engin *et al.* (2008b) studied the behavior of a single pile and pile group foundation using an embedded pile row, which showed similar behavior with the field test data for both a compression test and pullout test. The influence of pile spacing was also observed on the behavior of the pile group in terms of a load-displacement curve. It was found that as the spacing between piles increased, the load that the pile group could carry to produce the same settlement also increased. Lebeau (2008) employed a numerical modeling of a volume pile to analyze the influence of skin friction distribution on the behavior of a pile raft foundation. Using a load-displacement curve, the results of the volume pile were compared with a pile raft foundation modeled under axisymmetric conditions, where it was observed that the load-displacement curves were reasonably close to each other. The behavior of a pile group foundation can also be evaluated when it is subjected to excavation-induced soil movement. Analyzing a 4-pile group connected to a pile cap with different rigidity from centrifuge model tests, Choudhury *et al.* (2008) concluded that for a rigid pile cap, maximum negative bending moment was developed at the head of the pile, and it was larger compared to a flexible cap. Furthermore, larger pile head deflection was observed in a pile group with a flexible pile cap compared to a similar pile group with a rigid pile cap. Comodromos *et al.* (2009) optimized a foundation design for a bridge based on both experimental data and non-linear 3D analysis. They analyzed a relationship of load distribution with settlement and pile length for 2×2 and 3×3 pile group arrangements.

Chore *et al.* (2012) proposed a simplified finite element model for a parametric study of a laterally loaded pile group considering pile spacing, pile diameter, number of piles, and arrangement of piles on the responses of a pile group, where fair agreement between the proposed model and 3D finite element was observed. Chore *et al.* (2012) employed the finite element method to perform a parametric study of two groups of piles subjected to lateral loads incorporating the nonlinear behavior of soil. Sawant and Ladhane (2012) performed parametric studies of pile spacing, number of piles, different pile arrangements, and soil modulus on the dynamic response of a pile group using three-dimensional finite element analysis. Sawant and Shukla (2012) studied and compared solutions of laterally loaded piles between three-dimensional finite element analyses and a closed-form expression of the modulus of a subgrade reaction method with consideration of different combinations of soil and pile characteristics. Chore and Siddiqui (2013) employed the finite element method to analyze a piled raft foundation considering parametric studies of soil modulus, raft thickness, and different load patterns. Chore *et al.* (2014) employed three-dimensional finite element method to model a space frame pile foundation and soil system while the nonlinear behavior of soil was incorporated by idealizing the soil as nonlinear springs using a p-y curve along the lines. The three-dimensional finite element method was employed by Chore (2014) and Dode *et al.* (2014) to study a typical single storeyed building frame resting on a pile foundation and embedded in a cohesive soil with parametric studies in terms of number of piles, pile diameter, and pile spacing on the response of a superstructure. Doran and Seekin (2014) studied the lateral load carrying capacity of a designed wharf structure

considering soil-pile interaction effects for different soil conditions.

Very recently, Fattah *et al.* (2015) performed an experimental study to investigate the behavior of a piled raft system in different types of sandy soil. Wu *et al.* (2015) derived an analytical solution using a nonlinear softening model for the load transfer mechanism of a single axially-loaded pile, while the developed analytical solution was validated through a pile load test.

Even though a large number of previous works have studied pile raft and pile group foundations, most have focused on settlement or bearing capacity of a pile group with purely vertical loads and/or lateral loads. In addition, smaller numbers of piles, like 4 piles (2×2) or 9 piles (3×3), in the pile group foundations were investigated. There have been very few studies examining pile load distribution in a pile group foundation subjected to combined vertical load and large moment with consideration of a large number of piles in the pile group. Thus, the objective of this paper is to investigate the behavior of pile load distribution behavior for a pile group foundation subjected to vertical load and large moment by 3D finite element analysis. The numerical model corresponds with 49 piles (7×7) and 196 piles (14×14) in the pile group foundation for the physical model of a wind turbine. In this study, the special element, embedded pile in PLAXIS3D, is adopted to model a pile instead of using volume element in order to avoid numerical problems of mesh generation associated with a large number of piles and to reduce computational time. The behavior of a single pile case is first analyzed followed by a study of the behavior of a square pile group foundation of a wind turbine, which is subjected to a combined vertical load and large moment. A mathematical expression which describes the individual pile load distribution of the pile group obtained from finite element analysis is proposed.

2. Method of analysis

2.1 3 D Finite element software

In this study, PLAXIS3D (Brinkgreve *et al.* 2013) was employed to analyze a single pile and a pile group foundation for a wind turbine. This software is capable of analyzing stability and deformation problems in geotechnical engineering, including static and dynamic 3D nonlinear finite element analysis. In addition, PLAXIS3D is equipped with features to deal with various aspects of complex geotechnical structures including elasto-plastic deformation analysis of advanced soil models. Of particular interest is its ability to handle a problem of soil-structure interaction, where fully structural models are available, including plate elements, beam elements, and special elements called embedded piles, where it is intended to model piles in a pile group foundation.

2.2 Site classification

The soil profile considered in this study is located in southern Thailand. It consists of clay layers subdivided into four general types as shown in Fig. 2. The first layer is classified as very soft clay where its undrained shear strength, s_u and Young's modulus, E_u , increases linearly from elevation 0 m to elevation -15 m. The second layer is composed of medium stiff clay, which is located from elevation -15 m to -20 m. From elevation -20 m to -27 m, soil stratum is made up of stiff clay. The last layer comprises elevation -27 m to -35 m, which is classified as hard clay. The second to fourth layers have constant undrained shear strength, s_u and Young's modulus, E_u with different magnitudes. The ground water level (G.W.L.) is located 1.50 m below the ground surface.

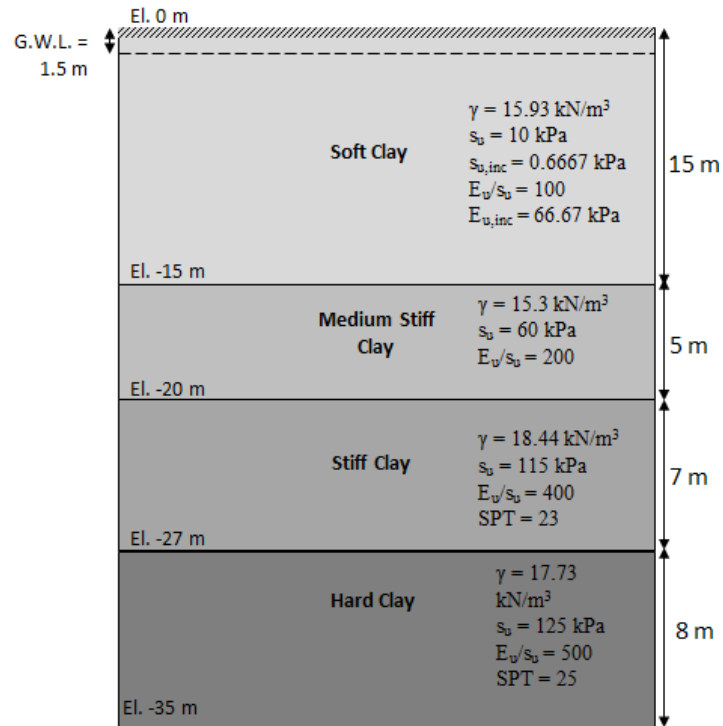


Fig. 2 Soil profile of a selected site

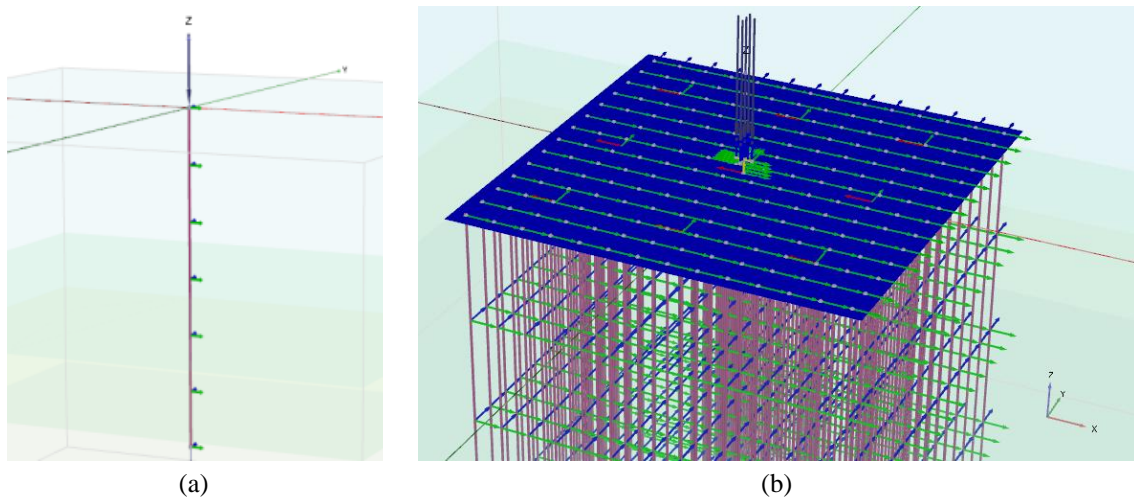


Fig. 3 Geometry and numerical models: (a) single pile; and (b) pile group foundation

For this study, the pile tip is designed to be located at the hard clay (elevation -27 m). The properties of each soil layer will be presented in a subsequent section of the paper.

2.3 Characteristics of 3D finite element model

2.3.1 Geometry model

Fig. 3 shows the geometry model of a single pile and pile group foundation for a wind turbine. For the case of a single pile, the geometry of a numerical model consists of two material components: (1) soil elements; and (2) single embedded pile elements. For the case of a pile group foundation, the geometry of a numerical model consists of four material components: (1) soil elements; (2) embedded pile elements; (3) plate element for pile cap; and (4) beam element for the load transfer.

The soils are discretized by the 10-noded tetrahedral element with three translational degrees of freedom per node. The plate elements modelling a pile cap form a 6-noded triangular element, where each node has three translational degrees of freedom and three rotational degrees of freedom. The formulations of plate elements are based on Mindlin’s plate theory (Bathe 1996). Piles are modelled using a special element called an embedded pile element (Engin *et al.* 2007, 2008a), which is a 3-noded line element with three translational degrees of freedom and three rotational degrees of freedom per node. The beam elements used to model the elements of the load transfer have the same nodes and same degrees of freedom as the embedded pile elements. Soil and the structural elements are schematically shown in Fig. 4.

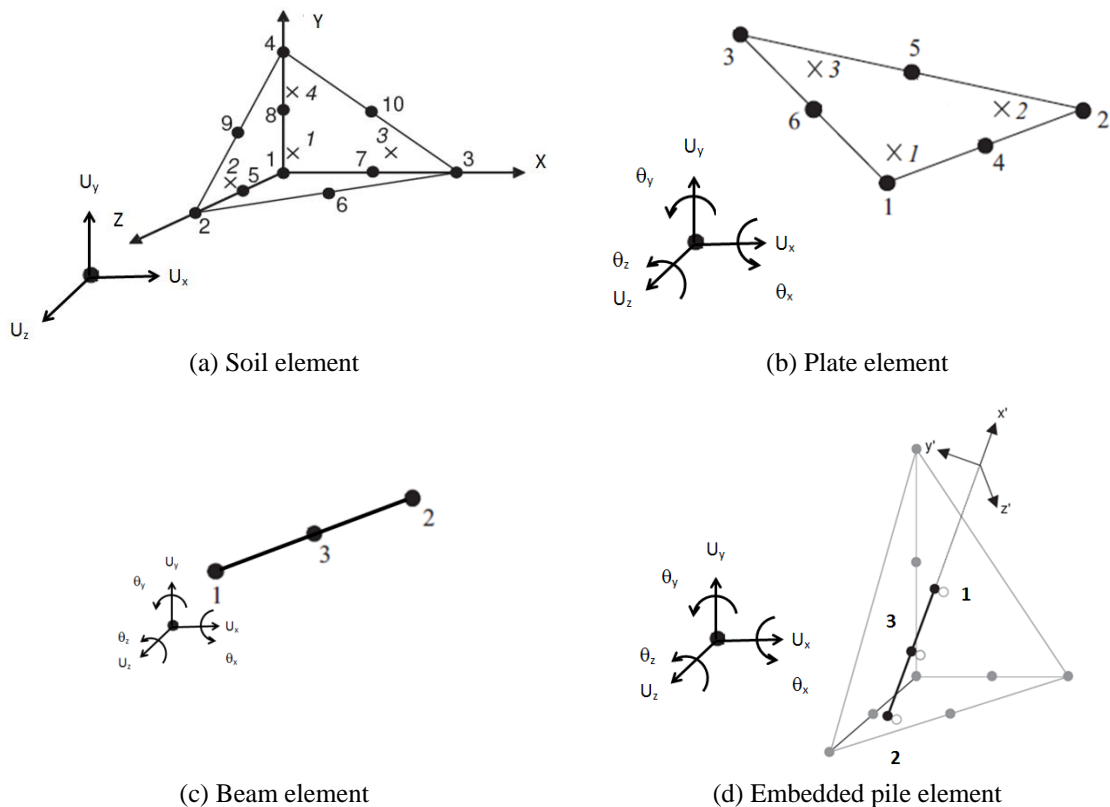


Fig. 4 Types of element and their degrees of freedom in PLAXIS3D (modified from Brinkgreve *et al.* 2013)

It should be noted that the plate element was selected to model a thick pile cap instead of using the solid element because the plate element allows a fully compatible connection with the embedded pile element since both elements have three translational degrees of freedom and three rotational degrees of freedom. If solid element and embedded pile element are used in the same numerical model, numerical problems may arise due to incompatibility in the rotational degree of freedom at the connection between a plate element and embedded pile element since the solid element has only three translational degrees of freedom. In addition, the plate element gives a comparable shear and bending responses of pile cap as compared to the solid elements since it is based on Mindlin's beam theory (Bathe 1996).

In this study, the plate element of a pile cap and the underlying soil are modeled to have a small gap (0.1 m) between them in order to simulate the problem of a pile group foundation, as shown in Fig. 5. This modeling is to avoid load transfer from the pile cap to the underlying soil. With this small gap, the vertical load and moment applied to the pile cap are transferred only to the pile group without any load sharing to the underlying soil. The connection between the plate element of the pile cap and embedded piles is a hinged connection in order to allow only vertical load transfer without transferring bending moment.

For a pile group foundation subjected to both a vertical load (F) and a moment (M_y), the rigid beam elements are used to transfer statically equivalent couple forces (C_y) for the applied moment (M_y), as schematically shown in Fig. 6. The vertical load (F) is also applied at the top center of this rigid beam elements. In the case of a purely vertical load, there are no couple forces in the finite element model.

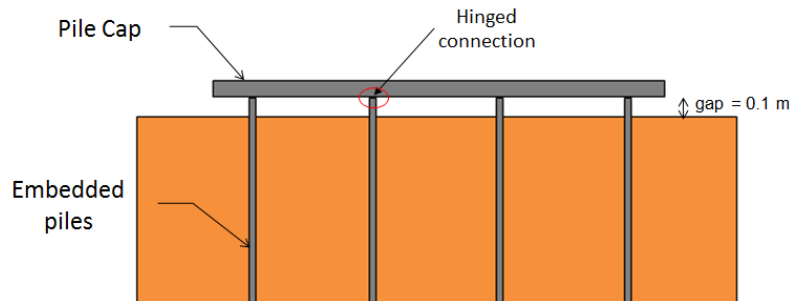


Fig. 5 Modeling techniques for connection between piles and pile cap

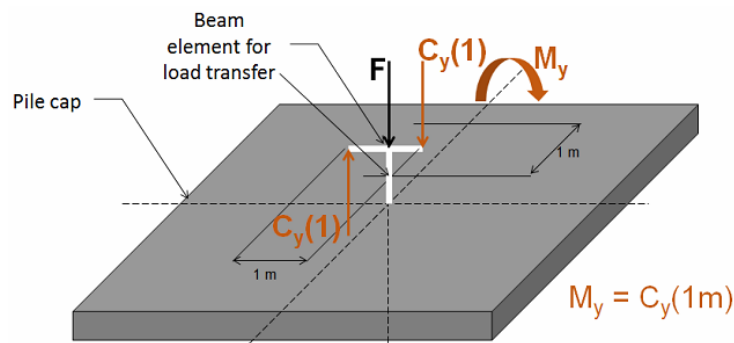


Fig. 6 Transfer mechanism of vertical load and moment

2.3.2 Material properties

The constitutive model used for all clay layers is Mohr-Coulomb material in an undrained condition and the associated flow rule, where it behaves as the elastic-perfectly plastic material. The Mohr-Coulomb model requires five input parameter including: (1) undrained Young's modulus (E_u); (2) Poisson's ratio ($\nu = 0.495$); (3) Undrained shear strength (s_u); (4) total friction angle ($\phi = 0$, total stress analysis); and (5) dilatancy angle ($\psi = \phi = 0$, associated flow rule). In an undrained loading analysis of the problem, the undrained type C is used, where the stiffness and shear strength are inputted as the total stress parameters in the finite element simulation. Soil parameters for each soil layer are shown in Table 1. The undrained shear strength of each clay layer is based on the field vane shear tests at the site, while the undrained Young's modulus is obtained from the empirical relation proposed by Duncan and Buchigami (1976).

The pile cap is modeled as a plate element with an elastic material that has large flexural and axial stiffness to ensure that it behaves as a rigid element. The beam elements for transferring couples force as applied moment are also rigid. Table 2 shows the material properties for the plate element modelling a pile cap.

In a pile group foundation, each pile has a diameter of 0.6 m and length of 27 m. In this paper, the piles are modelled using the special element called the embedded pile element developed by

Table 1 Material properties of each soil layer

Parameter	Symbol (Unit)	Soft clay	Medium stiff clay	Stiff clay	Hard clay
Material model	Model	Mohr-Coulomb	Mohr-Coulomb	Mohr-Coulomb	Mohr-Coulomb
Drainage type	Type	Undrained (C)	Undrained (C)	Undrained (C)	Undrained (C)
Unsaturated unit weight	γ_{unsat} (kN/m ³)	15.93	15.3	19.3	17.73
Saturated unit weight	γ_{sat} (kN/m ³)	15.93	15.3	19.3	17.73
Young's modulus	E_u (kN/m ²)	1,000	15,000	46,000	62,500
Poisson's ratio	ν	0.495	0.495	0.495	0.495
Undrained shear strength	s_u (kN/m ²)	10	60	115	125
Strength reduction factor	R_{inter}	0.67	0.67	0.67	0.67

Table 2 Material properties of plate element modelling pile cap

Parameter	Symbol	Unit	Value
Young's modulus	E	kN/m ²	2.54×10^7
Unit weight	γ	kN/m ³	24
Thickness	t	m	1.8
Poisson's ratio	ν	kN	0.2

Engin *et al.* (2007, 2008a) and validated for vertical loading (Engin *et al.* 2008b, Engin and Brinkgreve 2009) and lateral loading (Dao 2011). An embedded pile is a special beam element in any arbitrary direction that can cross a soil element. Although an embedded pile does not occupy volume, a particular volume around the pile (elastic zone) is assumed in which plastic soil behavior is excluded. The size of this elastic zone is based on the equivalent pile radius, R_{eq} . Through this parameter that is pre-defined in the material data set, an elastic zone around the pile is given, which makes the embedded pile element almost behave like a volume pile. It should be noted that installation effects of piles are not taken into account by this special element. Thus, piles with minimum soil disturbance should be used as bored piles.

This paper adopts the use of an embedded pile element to model the piles since it has many advantages over a volume pile. Firstly, the embedded pile element gives rise to a more efficient calculation time for the pile group. Because of a line element, there is less numerical complication in mesh generation of a pile group, particularly with a large number of piles. As a result, the total number of elements in the mesh is much smaller than the volume piles, resulting in an efficient time period for numerical calculations. In addition, since an embedded pile is a beam element, it can give the direct results of structural forces (axial and shear forces and moment) from the output. In contrast, an additional modeling technique is required to obtain structural forces in the case of a volume pile.

The embedded pile and soil interaction are modelled at the center rather than at the circumference. The embedded pile element interacts with the surrounding soil by means of special interface elements that include a pile skin resistance and pile foot resistance. The interface element is described as having an elastic-plastic model. A failure criterion is used to describe the behavior of the pile, whether it is in elastic or plastic behavior. In elastic behavior, the pile is allowed to have small displacement differences in the interface, while permanent slip in the interface between pile and soil can occur in the plastic behavior. For the interface to remain in elastic behavior, the shear stress is smaller than the maximum traction along the pile, and the end bearing force is also smaller than the maximum foot force. When those two conditions are not met, plastic behavior and permanent slip occur at the interface of the embedded pile element. The maximum traction along the pile is based on its shaft resistance force per unit length, while the maximum foot force is

Table 3 Material properties of embedded pile element

Parameter	Symbol	Unit	Value
Young's modulus	E	kN/m ²	2.54×10^7
Unit weight	γ	kN/m ³	24
Pile type		Massive circular pile	
Diameter	d	m	0.6
Skin resistance	Multi-linear		
		L (m)	T (kN/m)
		0.1	0.00
		15.1	25.26
		20.1	126.29
	27.1	164.18	
End-bearing resistance	F_{max}	kN	420.03

based on the end bearing capacity of the pile, where both values are defined by the user. It should be noted that the embedded pile material data set does not contain so-called ‘ p - y curves’ nor equivalent spring constants. In fact, the stiffness response of an embedded pile subjected to loading is the result of the specified pile length, equivalent radius, spacing, stiffness, and bearing capacity as well as the stiffness of the surrounding soil. More details of embedded pile formulation can be found in Engin *et al.* (2007, 2008a).

The properties embedded pile elements are summarized in Table 3. Interface roughness (R_{inter}) between the embedded pile and surrounding soil is assumed to be 0.67, according to typical values of adhesion factor between soil and pile. The side friction force and end bearing force developed in the embedded pile are controlled by their shaft resistance and end resistance, respectively. These limiting conditions are also shown in Table 3, which are based on static manual calculation of pile capacity. The shaft resistance per unit length varies linearly within each soil layer as specified by the multi-linear function, where a linear variation between the top and bottom interfaces of each soil layer is defined.

2.3.3 Creation process of numerical models

In PLAXIS3D, a graphical user interface (GUI) is employed to create numerical models of both a single pile and a pile group foundation. GUI allows a user to easily generate a 3D FE model consisting of soil model, structure model, loads, boundary condition, mesh generation, and analysis. It should be noted that the main concept of GUI in PLAXIS3D is that the soil and structure models are inputted separately, and then they are automatically combined.

In the step of soil model creation, the lateral sizes (x and y directions) of domain are inputted to be large enough that they do not affect the numerical solutions. Then, the borehole utility is used to input each soil layer with its elevation and material properties shown in Fig. 2 and Table 1, respectively. Elevation of the water table is also inputted in this step for pore water pressure calculations in the first state of analysis.

The next step corresponds to the creation of structure models, including all structural elements, loads, and boundary conditions. For piles, an embedded pile element with the material properties shown in Table 3 is created at one corner of the pile grid. For the case of a pile group foundation, the array function using this embedded pile is employed to automatically generate all embedded piles in the group. For the pile cap, the plate element with the material properties shown in Table 2 is created with a gap of 0.1 m above the ground surface (see Fig. 5). The purpose this gap is to avoid load transfer from the pile cap to the underlying soil resulting in the behavior of a pile group foundation instead of a pile raft foundation. The connection between the top of the embedded piles and plate element are defined as the hinge so as not to transfer any moment to the piles. Rigid beam elements are created as a T-shape for the load transfer structure (see Fig. 6). It should be noted that the connections of degrees of freedom for all structural elements are automatically generated, resulting in a completely compatible structural model. A vertical load and a couple of forces are created at the center and ends of the T-shape, respectively (see Fig. 6).

Boundary conditions are defined at external boundary planes using default displacement boundary conditions. Displacements of bottom planes are fully fixed in all directions. The boundary conditions of the external vertical planes are defined such that only normal displacements of the plane are zero, while the displacements in the other remaining directions are free. The remaining undefined external boundary planes such as the top ground surface are treated as a free surface where three directions of displacement are permitted to occur.

2.3.4 Mesh generation

After the soil and structural models, loads, and boundary are completely defined, a fully automatic mesh generation is performed, where the model geometry is divided into volume elements and compatible structure elements as described in Section 2.3.1. The mesh generation takes full account of the position of the geometry entities in the geometry mode so that the exact positions of soil layers, structures, and loads are accounted for in the finite element mesh. A local mesh refinement is then adjusted in the mesh generation of volume elements.

To optimize the accuracy and amount of time required to perform the load steps in 3D finite element simulation, the global coarseness is set to medium mesh refinement. Fig. 7 shows an example of mesh generation with medium mesh refinement for the case of a pile group foundation of a wind turbine. Automatic mesh generation is performed by PLAXIS3D, where tetrahedral elements and plate elements are created using the Delaunay algorithm to produce an unstructured mesh for the numerical model.

2.3.5 Finite element calculation

Each load step in PLAXIS3D is inputted as a stage of analysis. For the cases of a single pile and pile group foundation, the following stages of analysis are defined as follows:

- (1) The first stage of analysis corresponds to the initial stress generation, where the effective stress is calculated by using the K_0 procedure, while the pore water pressure is calculated following a hydrostatic condition. In this stage, all structural elements, loads, and boundary conditions are deactivated while only soil elements are present in the model.
- (2) For a pile group foundation, the second stage of analysis corresponds to the activation of all structural elements, including embedded piles, plate element, beams for load transfer, and boundary conditions. For a single pile case, only a single embedded pile and boundary conditions are activated.
- (3) Two load cases, including a vertical load and a vertical load and moment, are inputted for the third and fourth stages of analysis of a pile group foundation, respectively. Only a single load case of a vertical load is defined for a single pile case.
- (4) Once all stages are setup and defined, a nonlinear elastic-plastic deformation analysis is performed from the second stage to the last one. For each stage, an iterative procedure with an automatic load stepping control is employed, which is based on an accelerated initial stress method of an elastic stiffness matrix (Zienkiewicz 1977). The program will automatically use the most appropriate numerical procedure and proper selection of load steps to determine a nonlinear finite element solution with an optimum performance. All analyses employ the default numerical procedure, Picos, which is an efficient iterative solver that solves the system of sparse linear equations in parallel on multi-core processors. The implicit stress integration algorithm is used to obtain a stress increment at each integration point for known increments of strain. More details of Picos and stress integration scheme can be found in the manual of PLAXIS3D.

3. Results and discussions

3.1 Calculation of pile capacity

It should be noted that an estimation of ultimate pile capacity is necessary in order to obtain the

ultimate shaft resistance force and end bearing force to calculate the limiting shaft traction along the pile and tip force as input parameters for embedded pile elements. The ultimate bearing capacity of an individual pile can be computed using a conventional hand calculation as

$$Q_{ult} = Q_s + Q_E - W_p \quad (2)$$

$$Q_s = \sum (R_{inter} s_{ui} P_i L_i) \quad (3)$$

$$Q_E = (9s_{ub} + \sigma_v) A \quad (4)$$

where, Q_{ult} = the ultimate pile capacity
 Q_s = the ultimate shaft resistance
 Q_E = the ultimate end bearing force
 W_p = the weight of the pile
 P = the perimeter of pile layer i
 L = the length of pile layer i
 s_{ui} = undrained shear strength of soil layer i
 A = area of the pile
 s_{ub} = undrained shear strength of clay at the tip of pile
 σ_v = total overburden pressure at the tip of the pile

The allowable bearing capacity, Q_{all} is computed by dividing the sum of shaft resistance, Q_s and end bearing resistance, Q_E , by the factor of safety, FS , which is 2.5, then subtracting it by the weight of the pile, W_p . Table 4 summarizes the computed values of pile capacity.

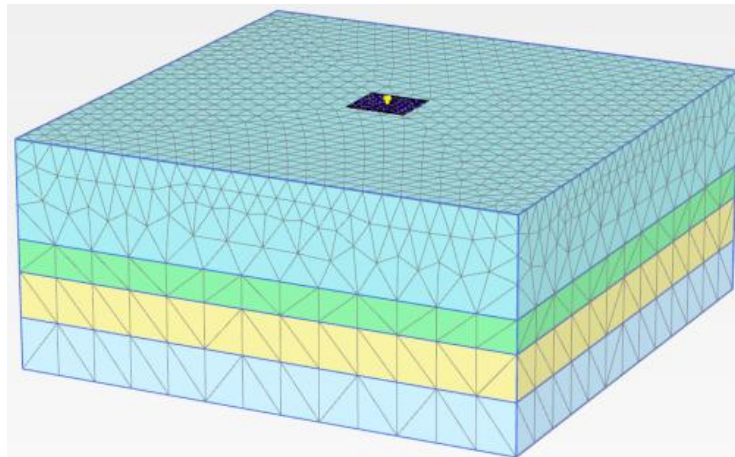


Fig. 7 Example of mesh generation for a pile group foundation of wind turbine

Table 4 Pile capacity calculation

Q_s (kN)	Q_E (kN)	W_p (kN)	Q_{ult} (kN)	Q_{all} (kN)
1584.96	420.03	183.22	1,821.78	618.78

Plastic stage analysis is performed for the cases of a single pile and pile group foundation subjected to vertical load and large moment. Results and discussions are presented in the next section.

3.2 Single pile case

Fig. 8 shows the load-displacement curve of the single pile case with 0.6 m pile diameter and 27.0 m pile length. The vertical axis of the plot, M_{stage} , represents the ratio of current applied load to the input load, F_{input} , where $F_{input} = 3000$ kN. It can be observed that the curve consists of two zones, elastic and plastic parts. At first, a linear relationship is observed in the range of applied load = 0 to 1500 kN. Beyond this load level, the plastic behavior is observed for a nonlinear relationship between M_{stage} and displacement. The load displacement curve does not show a clear limit state condition. However, the computed ultimate pile capacity is obtained from the last step of analysis as: $P_{ult} = 0.6904 \times 3000 = 2071$ kN. The pile capacity of finite element analysis is slightly higher than that of the hand calculation method, 1822 kN, shown in Table 4. As shown in Fig. 9, the mobilized end bearing force, 420 kN, also agrees very well with the value of hand calculation. The results indicate that the behavior of a single pile can be analyzed accurately using 3D finite element analysis with an embedded pile element. If the applied load is equal to the allowable pile capacity, 619 kN or $M_{stage} = 0.21$, the pile behavior is still within the elastic range.

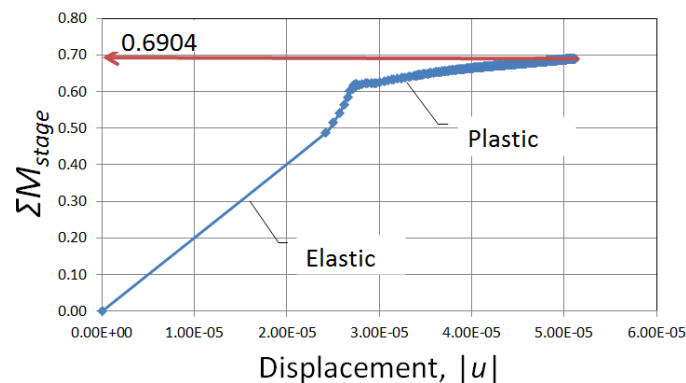


Fig. 8 Load-displacement curve of single pile

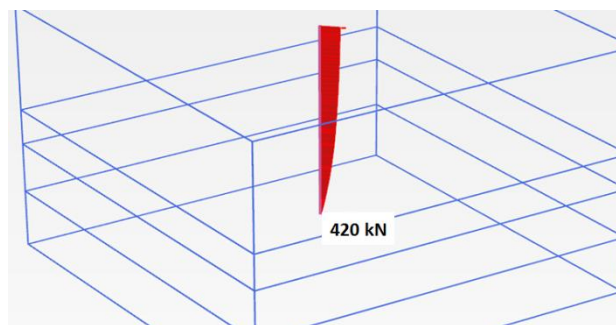


Fig. 9 Axial force distribution along single pile

3.2 Pile group foundation case

3.2.1 Summary of pile group foundation analysis

As shown in Fig. 10, the physical model of a wind turbine foundation is analyzed using a 3D finite element model by PLAXIS3D. The foundation of this large structure is subjected to combined vertical load and large moment. The weight of the structure and the pile cap represent the axial load, while the rotation of the blades represents a uniaxial moment with respect to y direction applied to the pile group foundation. In this study, the applied vertical load (V) is 3,500 kN (not including the weight of pile cap) and large moment (M_y) is 36,000 kN.m, according to the manufacturer of the wind turbine. The pile group is modeled with a fully rigid pile cap with piles having a diameter of 0.6 m. and a length of 27 m. Only a square pile arrangement for the pile group is considered in this study. The pile cap is assumed to have a thickness of 1.8 m, which is used to calculate its self-weight. The first study is to determine a square shape pile group foundation that satisfies the allowable pile capacity criterion, followed by the development of an equation that predicts the behavior of an individual pile force with respect to their positions in the pile group. Two analyses are employed in this study: (1) the classical method (e.g., Bowles 1988, Das 2014); and (2) 3D finite element analysis, PLAXIS 3D. The pile group foundation must satisfy the allowable pile capacity criterion when it is subjected to combined vertical load and large moment. Table 5 summarizes the results of analysis when a pile group foundation is subjected to combined vertical load and large moment. From this table, a 7×7 pile group is valid for the pile capacity criterion when the classical method is used. However, when it is verified by 3D finite element analysis, the pile group is no longer valid since the computed maximum pile force of 1,028 kN exceeds the allowable pile capacity, which is 619 kN.

Hence, another square pile group configuration is considered using 3D finite element analysis. Based on several simulations, it is found that the valid square pile group foundation is 14×14 . From the classical method of this case, the maximum force is 199 kN, while that of 3D finite

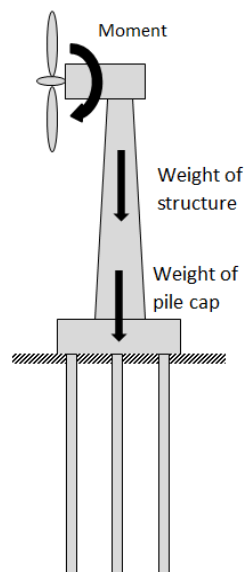


Fig. 10 Schematic diagram of a wind turbine

Table 5 Summary of analysis for combined vertical load and large moment

Case No.	Pile group	$P_{MAX,CA}$ (kN)	$P_{MAX,FE}$ (kN)	F (kN)	M_y (kN.m)	$P_{MAX,FE}/F$ (%)	Q_{all} (kN)
1	7 × 7	518	1,028	10,373	36,000	9.91	619
2	14 × 14	199	617	30,948	36,000	1.99	619

Remarks: $P_{MAX,CA}$ = Maximum pile force from classical analysis
 $P_{MAX,FE}$ = Maximum pile force from 3D finite element analysis
 F = total applied vertical load
 M_y = applied large moment in y direction

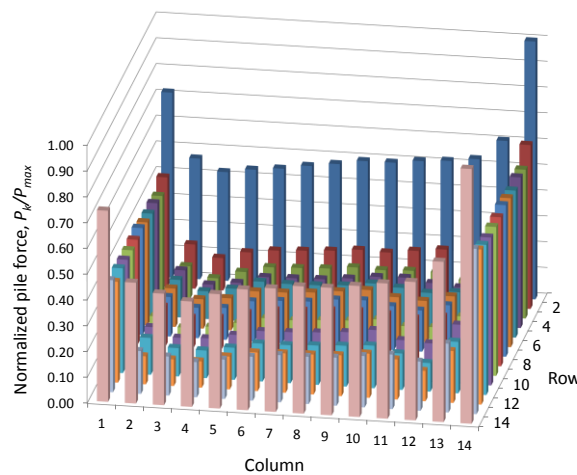


Fig. 11 3D Normalized pile force distribution of 14x14 pile group subjected to combined vertical load and large moment

element analysis is 617 kN. The large difference of these square pile group foundations is due to an abrupt increase of forces at the corner piles, where the maximum force is found at the overturning side as shown in Fig. 11. Employing 3D finite element analysis, a more realistic pile-soil interaction contributes to the behavior of the pile group. A corner pile on the overturning side carries 1.99% of the applied vertical load, which produces 3.98% of the total vertical load for both corner piles.

After analyzing the 14×14 pile group foundation subjected to combined vertical load and large moment, another load case is studied, a purely vertical load. This is the case when the wind turbine does not operate, but it is not the critical loading case. From Table 6, both pile group

Table 6 Summary of analysis for a purely vertical load

Case No.	Pile group	$P_{MAX,CA}$ (kN)	$P_{MAX,FE}$ (kN)	F (kN)	$P_{MAX,FE}/F$ (%)	Q_{all} (kN)
1	7 × 7	212	554	10,373	5.34	619
2	14 × 14	158	540	30,948	1.75	619

Remarks: $P_{MAX,CA}$ = Maximum pile force from classical analysis
 $P_{MAX,FE}$ = Maximum pile force from 3D finite element analysis
 F = total applied vertical load

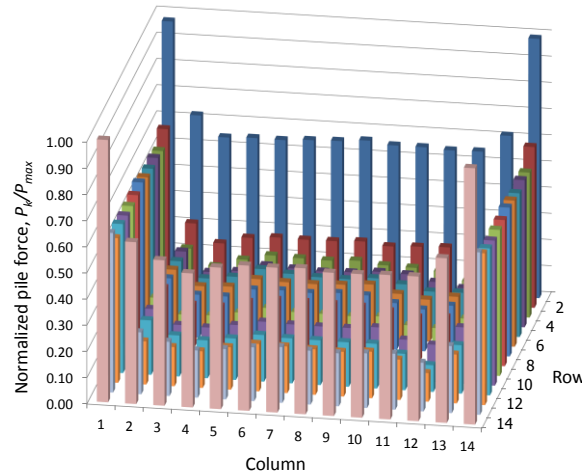


Fig. 12 3D Normalized pile force distribution of 14×14 pile group subjected to purely vertical load

configurations, 7×7 and 14×14, satisfy the pile capacity criterion. For a 14×14 pile group, it can be observed in Fig. 12 that the pile force distribution is symmetrical for both x - and y -axes. Moreover, the same observation with combined vertical load and large moment is noticed regarding the sudden increase in exterior piles, especially in corner piles due to mobilized shaft resistance, which justifies the findings of the previous works (Comodromos *et al.* 2009, Engin *et al.* 2008). The maximum force is observed at corner piles, where each pile carries 1.75% of the total applied vertical load.

3.2.2 Development of pile load distribution behavior for pile group foundation

After obtaining the results from finite element analysis, a mathematical expression for predicting the behavior of the pile group foundation is developed for pile forces in terms of the normalized location of an individual pile in the pile group. A biquartic interpolation is proposed to describe the pile force distribution in the pile group. This method is used to construct new data points by applying a fourth order (quartic) formula with two parameters, x and y . The pile force, P , can be expressed from the biquartic interpolation as

$$P = \sum_{j=0}^n \sum_{i=0}^n A_{ij} x^i y^j = A_{00} + A_{01}y + \dots + A_{(n)(n)}x^n y^n \quad (5)$$

where, A_{ij} represents the coefficient of the two dimensional variables;

k = an index of pile k

x_{\max} = the maximum pile position in x direction

y_{\max} = the maximum pile position in y direction

x and y are the normalized distances of the pile along x - and y -directions, respectively,

i.e., $x = x_k/x_{\max}$ and $y = y_k/y_{\max}$,

i and j = the power of x and y , respectively

n = the highest order power of the quartic equation = 4

Typically, the lower order forms, bicubic or biquadratic expressions, are used in image processing to reconstruct the image from a given set of data with minimum disparity (Takashi and Junho 2001). However, it can also be used in this study to predict the behavior of pile force distribution in the pile group foundation. From a general equation of the biquartic interpolation, 25 coefficients can be solved by the least square method (e.g., Sauer 2014, Walpole *et al.* 2002). However, a number of coefficients can be reduced based on the symmetry of the problem. The first case is the purely vertical load case, where pile forces are symmetrical on both axes. Hence, i and j should be only limited to powers of 0, 2, and 4 as shown in Eq. (6). For the square shape of a pile group configuration, the following constraints are enforced: $A_{20}=A_{02}$, $A_{40}=A_{04}$, and $A_{42}=A_{24}$. By enforcing those conditions with the least square method, the modified equation gives rise to 9 coefficients for a purely vertical load case by employing the biquartic equation in Eq. (6), where the optimal coefficients are not shown here since they are only applicable to the selected problem and cannot be used in design practice in other cases.

$$P = \sum_{j=0}^n \sum_{i=0}^n A_{ij} x^i y^j; i = j = 0, 2, 4 \tag{6}$$

Another considered case is a combined vertical load and large moment of a pile foundation for a wind turbine as described earlier. Since a uniaxial moment about y -axis is applied to the pile group foundation, the pile forces are only symmetrical along the y -axis. Hence, the values of j are limited to powers similar to those of the vertical load case, but the values of i are 0, 1, 2, and 4 as shown in Eq. (7). The modified equation for a square pile group foundation subjected to combined vertical load and large moment gives rise to 12 coefficients, where the optimal coefficients are not listed here as described previously.

$$P = \sum_{j=0}^n \sum_{i=0}^n A_{ij} x^i y^j; i = 0, 1, 2, 4; j = 0, 2, 4 \tag{7}$$

For comparison purposes between two loading cases, absolute values of coefficients are examined. Comparable coefficients can be observed when both variables are present in a term (A_{22} , A_{42} , A_{24} , and A_{44}) owing to the symmetrical property along the y -axis. On the other hand, when large moment is applied about the y -axis, it is found that pile forces are larger along the x -axis than that along the y -axis, hence $A_{20} > A_{02}$ n along the x -axis.

The results of the proposed biquartic expressions are compared to the data obtained from finite element analysis. Strips of rows and columns from the pile group foundation are chosen for comparison as shown in Fig. 13. ‘ R ’ represents the piles in the row, ‘ C ’ represents the piles in the column, subscript ‘ e ’ means exterior piles, and subscript ‘ c ’ means central piles. The load distribution behavior is investigated by considering two normalized plots. For subplots in Figs. 14 and 15, the horizontal axis represents either $A_{40} > A_{04}$. Moreover, the presence of $i = 1$ gives rise to the unsymmetrical pile force distributor the x -position of each pile, x_k divided by the maximum position, x_{max} of the exterior pile of the group, or the y -position of each pile, y_k divided by the maximum position, y_{max} , of the exterior pile of the group, giving rise to the range of -1.0 to 1.0. Moreover, the vertical axis represents the ratio of pile load, P_k , to the computed maximum pile load, P_{max} . The symbols correspond to the computed normalized pile forces from finite element analysis, while the dash lines are the predicted values from the biquartic expression. Similar trends can be observed between predicted values and computed values, where exterior rows and columns

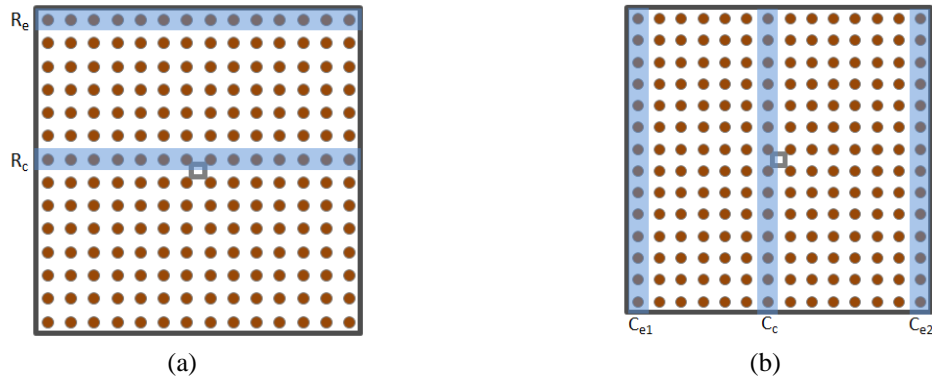


Fig. 13 Locations of pile used for comparisons

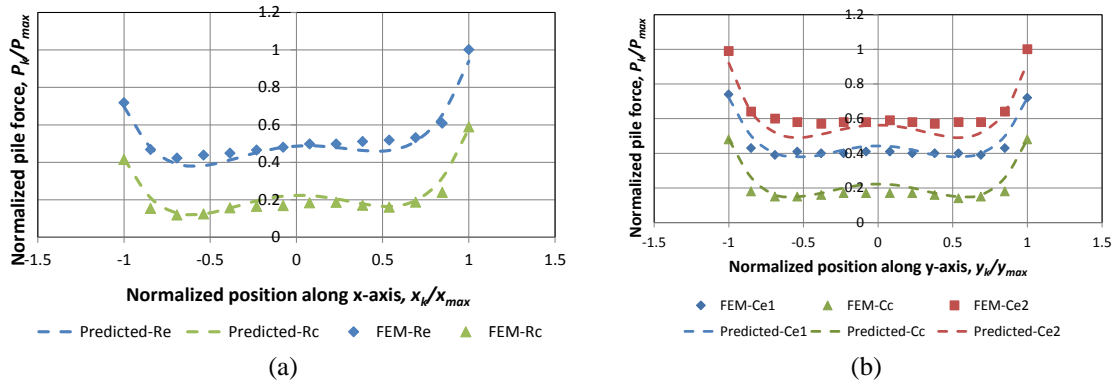


Fig. 14 Comparison of pile load distribution for combined vertical load and large moment: (a) x_k/x_{max} ; (b) y_k/y_{max}

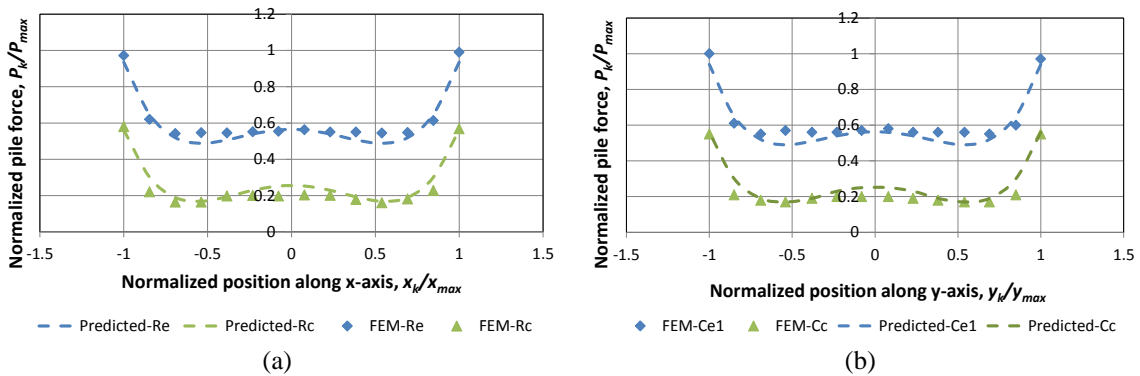


Fig. 15 Comparison of pile load distribution for purely vertical load: (a) x_k/x_{max} ; (b) y_k/y_{max}

show larger pile forces compared to the central piles. In addition, the highest pile force happens at the corner piles. For the case of combined vertical load and large moment, maximum pile force happens at the overturning side. For a purely vertical load case, symmetrical behavior along both

axes is observed. Considering a strip of either row or column and the position of this strip, either exterior or center, a two-curvature trend is always present. This result indicates that maximum pile forces occur at corner piles, and then the distribution of the pile force decreases when the piles are located at the middle. However, it increases again at the center right below the applied load.

The coefficient of determination (R^2) is used to measure how good the computed values from finite element analysis correlate with the modeled (predicted) values from the biquartic expression. Figs. 16 and 17 show a comparison between computed pile forces of finite element analysis and those of biquartic interpolation. Generally, most of the data points are close to the equality line, which means that the normalized pile forces from finite element analysis and biquartic expressions agree well with each other. The R^2 value for the cases of combined vertical load and large moment and purely vertical load are 94.28% and 94.66%, respectively. These values indicate that the biquartic expression can accurately predict the load distribution behavior of a pile group foundation subjected to either combined vertical load and large moment or purely vertical load.

It can be observed in both figures that there is a cluster of data divided into three parts including middle piles, exterior/edge piles, and corner piles. For both cases, the middle piles show a similar trend and have the smallest pile forces among the clusters. Normally, they range from 10% to 30% of the maximum pile force. On the other hand, pile forces in the exterior/edge piles are second in rank, which have the largest pile force. Different trends can be observed for both cases, where exterior pile forces for combined vertical load and large moment are more scattered compared to those of the purely vertical load case. This is due to the variability in the coefficients for the combined loading cases. On the other hand, additional constraints are enforced for predicting the pile forces of the purely vertical load case to ensure the symmetrical properties on both axes. Hence, the proportion of pile forces normalized with the maximum pile force ranges between 40% and 65% for combined loading, while that of the purely vertical load case ranges between 50% and 65%. As expected, for combined vertical load and large moment, two piles in the corner piles have lower values compared to other corner piles on the overturning side. On the other hand, all corner piles for the purely vertical load case have similar values.

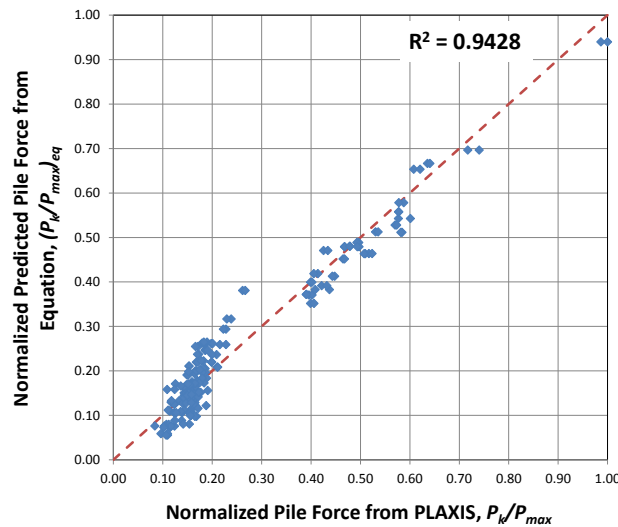


Fig. 16 Correlation between computed data and predicted value of pile group subjected to combined vertical load and large moment

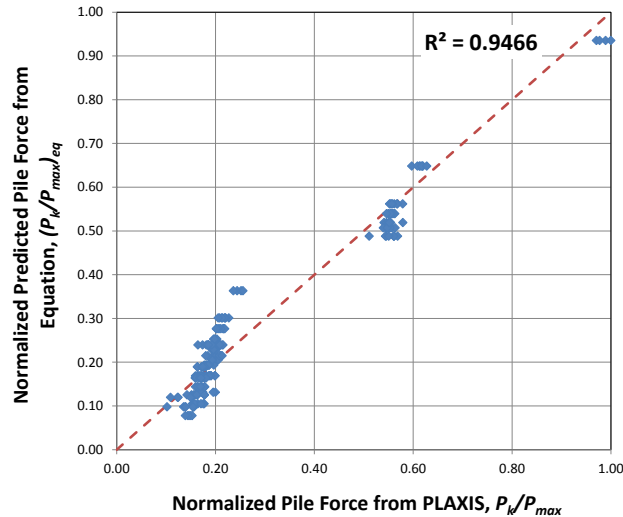


Fig. 17 Correlation between computed data and predicted value of pile group subjected to purely vertical load

4. Conclusions

This paper presents numerical investigations of 3D finite element modeling of a square pile group foundation for a wind turbine subjected to combined vertical load and large moment. Numerical studies are employed by 3D finite element analysis for both a single pile and pile group using an embedded pile element. Instead of a modeling pile as volume elements, an embedded pile element makes it possible to efficiently analyze a large number of piles in a pile group foundation such as a 7×7 or 14×14 pile groups. The main results of analyses are concentrated on pile load distribution with respect to the location of the individual pile. The accuracy of the embedded pile element is validated by comparing the results of a single pile from the 3D finite element analysis and conventional manual calculation.

It can be concluded that the use of the embedded pile element for a single pile to describe the behavior at the limit state is accurate and comparable to the manual method. The load distribution behavior of a square pile group foundation for a wind turbine is also analyzed for two cases: a purely vertical load and combined vertical load and large moment. It can be established that the present classical method that predicts the behavior of a pile group foundation may not be sufficient as this method leads to more of an underestimation of pile loads than those of more realistic 3D finite element analyses. Moreover, it produces a smaller number of piles compared to the finite element analysis that is unsafe in design practice. The fundamental reasons why there are significant differences between the results using the classical method and finite element analysis are that the classical method assumes: (1) a linear settlement of a rigid pile cap; (2) each pile represented by a spring with the same stiffness without settlement at its tip; and (3) no interaction between adjacent springs or no pile group effect. As a result, these assumptions give rise to the linear pile force distribution in the classical method. On the other hand, there are no assumptions used in the finite element analysis, where the pile group effect and settlement of each pile at its tip are fully taken into consideration in the finite element analysis. Hence, a more realistic behavior of nonlinear pile force distribution was predicted by finite element analysis.

It was found that for both cases of loading, a two-curvature trend of pile force distribution is present, which means the maximum pile force that happens at the corner piles decreases as the location of the pile gets closer to the center but increases again below the applied vertical load. The fourth (4) order polynomial expressions derived from biquartic interpolation is proposed to describe and predict the pile forces in terms of the normalized location of each pile in the pile group. The coefficient of determination, R^2 , for the case of a purely vertical load and combined vertical load and large moment are 94.66% and 94.28%, respectively. This high accuracy suggests that the proposed expressions can accurately predict the load distribution behavior for both cases.

It should be noted that further investigations regarding classical linear pile load distribution based on the rigid base assumption should be conducted due to discrepancies found when finite element analyses are performed. Moreover, parametric studies, including soil properties, pile diameter, pile spacing, pile length, and other pile group configurations, should also be performed in the future by 3D finite element models in order to have a better understanding of pile load distribution for a general pile group foundation. As a result, the biquartic expressions proposed in this study will be generalized and applied for the optimal design of a pile group foundation considering a more realistic pile force distribution instead of linear pile force distribution assumed in classical calculations.

References

- Bathe, K.J. (1996), *Finite Element Procedures*, Prentice-Hall, New Jersey, USA.
- Bowles, J.E. (1988), *Foundation Analysis and Design*, McGraw-Hill, Singapore.
- Brinkgreve, R.B.J., Engin, E. and Swolfs, M.W. (2013), *Plaxis 3D 2013 Manual*, A.A. Balkema Publishers, The Netherlands.
- Chore, H.S. (2014), "Interactive analysis of a building frame resting on pile foundation", *Coupled Syst. Mech., Int. J.*, **3**(4), 367-384.
- Chore, H.S. and Siddiqui, M.J. (2013), "Analysis of the piled raft for three load patterns: A parametric study", *Coupled Syst. Mech., Int. J.*, **2**(3), 289-302.
- Chore, H.S., Ingle, R.K. and Sawant, V.A. (2012), "Parametric study of laterally loaded pile groups using simplified F.E. models", *Coupled Syst. Mech., Int. J.*, **1**(1), 1-7.
- Chore, H.S., Ingle, R.K. and Sawant, V.A. (2014), "Non linear soil structure interaction of space frame pile foundation-soil system", *Struct. Eng. Mech., Int. J.*, **49**(1), 95-110.
- Choudhury, D., Shen, R.F. and Leung, C.F. (2008), "Centrifuge model study of pile group subject to Adjacent excavation", *Proceedings of GeoCongress 2008*, New Orleans, LA, USA, pp. 141-148.
- Comodromos, E.M., Anagnostopoulos, C.T. and Georgiadis, M.K. (2003), "Numerical assessment of axial pile group response based on load test", *Comput. Geotech.*, **30**(6), 505-515.
- Comodromos, E.M., Papadopoulou, M.C. and Rentzeperis, I.K., (2009), "Pile foundation analysis and design using experimental data and 3-D numerical analysis", *Comput. Geotech.*, **36**(5), 819-836.
- Dao, T.P.T. (2011), *Validation of PLAXIS Embedded Piles For Lateral Loading*, Master of Science Thesis; Delft University of Technology, The Netherlands.
- Das, B.M. (2014), *Principle of Foundation Engineering*, (8th Ed.), Cengage Learning, Boston, MA, USA.
- Dode, P.A., Chore, H.S. and Agrawal, D.K. (2014), "Interaction analysis of a building frame supported on pile groups", *Coupled Syst. Mech., Int. J.*, **3**(3), 305-318.
- Doran, B. and Seckin, A. (2014), "Soil-pile interaction effects in wharf structures under lateral loads", *Struct. Eng. Mech., Int. J.*, **51**(2), 267-276.
- Duncan, M.J. and Buchignani, A.L. (1976), *An Engineering Manual for Settlement Studies*, University of California, Berkeley, CA, USA.
- Engin, H.K. and Brinkgreve, R.B.J. (2009), "Investigation of Pile Behaviour Using Embedded Piles",

- Proceedings of the 17th International Symposium on Numerical Models in Geotechnical Engineering*, Alexandria, Egypt, October.
- Engin, H.K., Septanika, E.G. and Brinkgreve, R.B.J. (2007), "Improved embedded beam elements for the modelling of piles", *Proceedings of the 10th International Symposium on Numerical Models in Geotechnical Engineering*, Rhodes, Greece, April.
- Engin, H.K., Septanika, E.G., Brinkgreve, R.B.J. and Bonnier, P.G. (2008a), "Modeling piled foundation by means of embedded piles", *Proceedings of the 2nd International Workshop on Geotechnics of Soft Soils - Focus on Ground Improvement*, University of Strathclyde, Glasgow, Scotland, September.
- Engin, H.K., Septanika, E.G. and Brinkgreve, R.B.J. (2008b), "Estimation of pile group behavior using embedded piles", *Proceedings of the 12th International Conference of International Association for Computer Methods and Advances in Geomechanics (IACMAG)*, Goa, India, October, pp. 3231-3238.
- Fattah, M.Y., Yousif, M.A. and AlTameemi, S.M.K. (2015), "Effect of pile group geometry on bearing capacity of piled raft foundations", *Struct. Eng. Mech., Int. J.*, **54**(5), 829-853.
- Lebeau, J.S. (2008), "FE-analysis of piled and piled raft foundations", Ph.D. Thesis; Graz University of Technology, Austria.
- Mandolini, A., Russo, G. and Viggiani, C. (2005), "Pile foundations: experimental investigations, analysis and design", *Proceedings of the XVI International Conference on Soil Mechanics and Geotechnical Engineering*, Osaka, Japan, September, pp. 177-213.
- Sauer, T. (2014), *Numerical Analysis*, Pearson Education Limited, UK.
- Sawant, V.A. and Ladhane, K.B. (2012), "Dynamic response of pile groups in series and parallel configuration", *Struct. Eng. Mech., Int. J.*, **41**(3), 395-406.
- Sawant, V.A. and Shukla, S.K. (2012), "Can finite element and closed-form solutions for laterally loaded piles be identical?", *Struct. Eng. Mech., Int. J.*, **43**(2), 239-251.
- Takashi, S. and Junho, S. (2001), "Interpolation of one- and two-dimensional images with pixelwise photon number conservation", *Astronom. Soc. Japan*, **53**, 361-380.
- Walpole, R.E., Myers, R.H., Myers, S.L. and Ye, K. (2002), *Probability & Statistics for Engineering and Scientists*, (7th Ed.), Prentice Hall, NJ, USA.
- Wu, Y., Liu, J. and Chen, R. (2015), "An analytical analysis of a single axially-loaded pile using a nonlinear softening model", *Geomech. Eng., Int. J.*, **8**(6), 769-781.
- Zienkiewicz, O.C. (1977), *The Finite Element Method*, McGraw-Hill, USA.